Signaling interactions of rapamycin combined with erlotinib in cervical carcinoma xenografts

Diana C. Birle[1] and David W. Hedley[1,2]

[1]Division of Applied Molecular Oncology, Ontario Cancer Institute, University of Toronto; [2]Department of Medical Oncology and Hematology, Princess Margaret Hospital, Toronto, Ontario, Canada

Abstract

Clinical trials using rapamycin analogues or HER1/epidermal growth factor receptor (EGFR) inhibitors show that each class of agent has activity against a range of human solid tumors. Because blockade of mitogen-activated protein kinase signaling occurs following HER1/EGFR inhibition in some cell types, we tested the combination of rapamycin and erlotinib in SiHa, Me180, and CaSki human cervical carcinomas xenografts in severe combined immunodeficient mice. In tissue culture, all three cell lines showed decreased phosphorylated S6 ribosomal protein and decreased phosphorylated extracellular signal-regulated kinase (ERK) following treatment with rapamycin and erlotinib, respectively. In SiHa tumors, suppression of phosphorylated S6 was induced by either drug alone, whereas phosphorylated ERK decreased with erlotinib, and enhancement of these effects was obtained with the combination. Continuous treatment of xenografts for 3 weeks led to significant tumor growth delay compared with vehicle control for rapamycin as single agent (P = 0.003) and greater for the combination (P = 0.04 versus rapamycin). Significant antiangiogenic effect was obtained in SiHa xenografts using the drugs together (measured by microvascular density and vascular endothelial growth factor plasma levels) but not for the single agents. Me180 and CaSki xenografts showed significant growth delay with rapamycin but not with erlotinib. Erlotinib treatment resulted in decreased phosphorylated ERK, associated with enhanced suppression of phosphorylated S6 and improved growth delay in Me180 but not in CaSki tumors. These results support the further clinical investigation of rapamycin and EGFR inhibitor combinations in anticancer therapy but highlight the problem of intertumoral heterogeneity in the prediction of *in vivo* response. [Mol Cancer Ther 2006;5(10):2494–502]

Introduction

Aberrant signaling pathways are responsible for the features of cancer: unregulated growth, suppression of apoptosis, tumor angiogenesis, invasion, and metastasis. Consequently, a large effort is being made to develop novel agents that selectively target signaling elements for the treatment of cancer. Despite some clinical successes, response rates to single agents usually occur only in a minority of cancer patients and are typically incomplete. Given that cancers progress through multiple genetic abnormalities and the complexity of the interdependent signaling pathways, a combination of molecular directed drugs seems legitimate. The challenge would be then to rationally develop a mix of signaling inhibitors with enhanced anticancer activity and acceptable toxicity.

Excessive signaling through epidermal growth factor receptor (EGFR) due to receptor overexpression, autocrine stimulation, or activating mutations occurs in an extensive range of tumors and correlates with worse prognosis, thus justifying the efforts directed to inhibit its activity (1–3). Clinical trials using EGFR inhibitors, such as erlotinib, have shown partial responses or stabilization in various types of EGFR-positive tumors, with relatively mild side effects (1, 2).

The mammalian target of rapamycin (mTOR) plays critical roles in growth, differentiation, proliferation, migration, and survival (4, 5). It is an atypical serine-threonine kinase member of phosphatidylinositol kinase–related kinases family that acts as a sensor for the level of growth factors, nutrients, ATP, and oxygen (4–9). In response to these stimuli, mTOR regulates the activity of p70S6K and 4E-BP/PHAS, which have essential roles in ribosome biogenesis and cap-dependent translation via S6 ribosomal protein and eIF-4E, respectively (5, 6). mTOR also regulates other cellular processes, including cell-cycle proteins and RNA polymerases, protein phosphatases, hypoxia-inducible factor-1α, and vascular endothelial growth factor (VEGF) signaling (4–6, 8–10). Progress has been made recently understanding the interactions of mTOR, particularly within the phosphatidylinositol 3-kinase (PI3K)/protein kinase B (PKB) pathway, with the identification of several key modulators, including TSC1/2 and Rheb (4, 5, 11, 12). Rapamycin, a natural macrolide antibiotic, is an exquisitely specific inhibitor of mTOR downstream signaling (4, 5, 8). It has antiproliferative effects against a broad range of tumor cell lines and

Received 12/2/05; revised 6/23/06; accepted 8/16/06.

Grant support: National Cancer Institute of Canada using funds raised by the Terry Fox Run.

The costs of publication of this article were defrayed in part by the payment of page charges. This article must therefore be hereby marked advertisement in accordance with 18 U.S.C. Section 1734 solely to indicate this fact.

Requests for reprints: David W. Hedley, Department of Medical Oncology and Hematology, Princess Margaret Hospital, 610 University Avenue, Toronto, Ontario, Canada M5G 2M9. Phone: 416-946-2262; Fax: 416-946-6546. E-mail: david.hedley@uhn.on.ca

doi:10.1158/1535-7163.MCT-05-0504

antiangiogenic properties that translated into tumor growth inhibition in animal models (4, 12–16). This prompted the development of several analogues for testing as anticancer drugs (4).

Growth factors induce activation of tyrosine kinase receptors and consequently can signal through both PI3K/PKB/mTOR and mitogen-activated protein kinase (MAPK) pathways (2, 3, 5, 17). These pathways have multiple cross-connections at several levels, such as tuberin, p70S6K, and 4E-BP1 as illustrated in Fig. 1 (5, 10, 13, 17–29). p70S6K is believed to be the principal kinase for S6 ribosomal protein, and its activity correlates well with S6 phosphorylation (5, 6, 25). Besides experimental studies, immunohistochemical analysis of clinical samples is consistent with the dual activation model for p70S6K (30). The activation of p70S6K is triggered by the hierarchical phosphorylation of at least eight sites (5, 6, 31). Phosphorylated extracellular signal-regulated kinase (ERK) seems to be involved especially in the initial steps of activation, whereas mTOR-sensitive phosphorylation sites count for full activation of p70 (23–25, 31). S6 ribosomal protein represents the main substrate of the two isoforms of p70S6K (S6K1 and S6K2), and its activation is therefore sensitive to rapamycin. Based on these considerations, we hypothesized that simultaneous inhibition of mTOR and MAPK pathways would result in enhanced inhibition of S6 activation, in addition to other synergistic effects expected when targeting two major pathways that display extensive cross-talk. Furthermore, there is an extensive literature reporting the antiangiogenic effects of rapamycin and EGFR inhibitors (2, 10, 12–14, 32–34). VEGF, the key molecule for angiogenesis, is mainly regulated through hypoxia-inducible factors. Although hypoxia-inducible factor is controlled differently during normoxia versus hypoxia, dual regulation from PI3K/PKB/mTOR and MAPK is required at all times (7, 9, 10, 13, 17, 27–29, 31, 35). Up-regulation and modulation of hypoxia-inducible factor protein levels is considered to be achieved through PKB/mTOR, whereas its transactivation relies essentially on MAPK, which recruits the coactivators (9, 28, 29). These interactions were examined in a series of human cervical cancer xenografts.

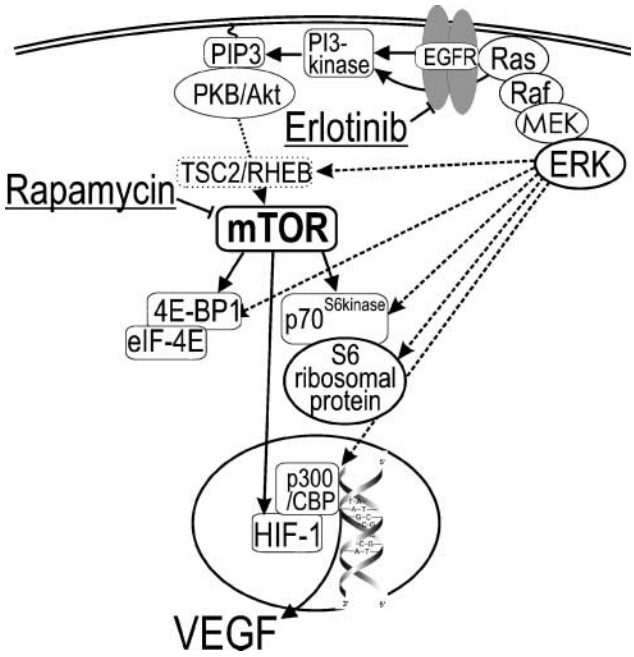

Figure 1. Schematic showing downstream targets of signaling triggered by EGFR activation and extensive cross-talk between mTOR and MAPK pathways. *MEK,* MAPK/ERK kinase; *HIF-1,* hypoxia-inducible factor-1.

Materials and Methods

Reagents and Antibodies

Erlotinib was obtained from OSI Pharmaceuticals, Inc. (Uniondale, NY) and dissolved in DMSO at 5 mg/mL freshly for each treatment. Rapamycin was purchased from Calbiochem (San Diego, CA). EGF was from Sigma (St. Louis, MO), and UO126 was from Cell Signaling Technology (Beverly, MA). The following antibodies were purchased from Cell Signaling Technology: phosphorylated ERK Thr^{202}/Tyr^{204} monoclonal E10 for immunofluorescence staining; phosphorylated ERK polyclonal for Western blots; phosphorylated S6 ribosomal protein polyclonals to Ser^{235}/Ser^{236}, Ser^{240}/Ser^{244}; polyclonal phosphorylated PKB Ser^{473}; and polyclonal cleaved caspase-3. Rabbit monoclonal anti-phosphorylated p70S6K Thr^{389} was from Epitomics (Burlingame, CA). Anti-α-tubulin was from Oncogene (Cambridge, MA), CD31 was from BD Biosciences (San Diego, CA), and Ki-67 (clone MIB-1) was from DAKO (Glostrup, Denmark).

Cell Proliferation Assay

For testing the antiproliferative effects of the drugs, SiHa cells were cultured in 96-well plates at 3,000 per well in 100 μL complete medium. The drugs were added in various concentrations, and after 48 hours, according to the manufacturer's instructions, the viable cell number was determined using a colorimetric method based on the cellular bioreduction of the tetrazolium compound 3-(4,5-dimethylthiazol-2-yl)-5-(3-carboxymethoxyphenyl)-2-(4-sulfophenyl)-2H-tetrazolium (MTS) into a soluble colored formazan product (CellTiter 96 Aqueous One Solution Cell Proliferation Assay, Promega Corp., Madison, WI).

Cell Treatment and Western Blots

The human cervical squamous cell carcinoma cell lines SiHa, Me180, and CaSki were obtained from the American Type Culture Collection (Manassas, VA) and cultured in α-MEM, McCoy's medium, and RPMI 1640, respectively, all supplemented with 10% fetal bovine serum. Cells were plated in 100-mm dishes at appropriate concentration and treated for the indicated periods. The cells were washed twice in ice-cold PBS, and 650 μL of lysis buffer [50 mmol/L HEPES (pH 8.0), 10% glycerol, 1% Triton X-100, 150 mmol/L NaCl, 1 mmol/L EDTA, 1.5 mmol/L

$MgCl_2$, 100 mmol/L NaF, 10 mmol/L NaP_2O_7, 1 mmol/L Na_3VO_4, supplemented with protease inhibitor cocktail from Roche Diagnostics, Mannheim, Germany] were added to each dish; lysis was conducted for 1 hour on ice. Equivalent amounts of protein (assayed with bicinchoninic acid protein assay from Pierce PerBio, Rockford, IL) were separated by SDS-PAGE gels. Proteins were transferred to polyvinylidene difluoride membranes (Millipore, Bedford, MA) and probed with the appropriate antibodies according to the manufacturer's instructions. Detection was conducted using enhanced chemiluminescence kit (Amersham Biosciences, Buckinghamshire, United Kingdom).

Xenografts

Animal experiments were done according to institutional guidelines for animal welfare. Cell suspension (0.1 mL, containing $\sim 5 \times 10^5$ cells) was injected into the left gastrocnemius muscle of severe combined immunodeficient mice. After ~ 2 weeks, the tumors became visible and the tumor plus leg diameter was measured between 7.5 and 8.5 mm. At this point, the mice were randomly assigned to four groups of five mice. The treatments included rapamycin given twice weekly at 2.5 mg/kg and erlotinib given daily at 10 mg/kg. Both drugs were dissolved in DMSO and given by i.p. injection. For the combined treatment, rapamycin was given first and erlotinib 1 hour later. The control group was injected with the same amount of DMSO as was used as a vehicle for the double-treated animals. Animal weight and tumor measurements were made every 2nd day. At the end of treatment, the mice were killed and the tumors were excised and processed as follows: each tumor was dissected from the surrounding tissues and cut into several pieces (approximately $3 \times 3 \times 3$ mm), which were randomized and split in three groups. Pieces from first group were placed in OCT embedding medium (Miles, Inc., Elkhart, IN) and snap frozen in liquid nitrogen; pieces from the second group were fixed in formalin for 24 hours and paraffin embedded. The remaining tissues were lysed 1 hour on ice in 1.5 mL lysis buffer as for the cell lysates.

To examine the short-term effects of drugs, 15 SiHa tumors were allowed to grow 13 to 14 mm in tumor plus leg diameter. Mice were randomized in four groups: three for controls and four in each rapamycin, erlotinib, and rapamycin plus erlotinib groups. DMSO and drugs were given as above; tumors were excised 60 minutes later and processed as above.

Plasma VEGF was measured using an ELISA assay (R&D Systems, Minneapolis, MN) that recognizes both human $VEGF_{165}$ and $VEGF_{121}$ and, at 50 ng/mL, does not cross-react with mouse VEGF. To allow for effects of the individual tumor sizes on the plasma levels of VEGF, we expressed these as (pg/mL) / mm^3 tumor volume $\times$ 100 in addition to the actual plasma concentrations.

Immunofluorescence Staining

Serial sections from the SiHa tumors were cut, and one was stained with H&E for selecting the tumoral areas on which the further image analysis was to be done. The other sections were labeled with primary antibodies against (*a*) phosphorylated S6 (Ser^{235}/Ser^{236}) and phosphorylated ERK, (*b*) CD31 and cleaved caspase-3, and (*c*) Ki-67. Secondary antibodies used alone were control for nonspecific background. All sections were counterstained with 1 μg/mL 4′,6-diamidino-2-phenylindole (DAPI) to outline the nuclear area.

Computerized Image Analysis

Tissue sections were examined using a fluorescence image analysis system (Microcomputer Imaging Device, Imaging Research, Inc., St. Catharines, Ontario, Canada) equipped with a cooled CCD camera (Quantix, Photometrics, Tucson, AZ). The analysis included the entire viable tumoral area identified on the slide using a scanning autostage to create composite images of individual fields at 20× (2.24 mm^2) as described previously (32). The tumoral map in which the actual measurements were made was initially determined using the H&E sections and then carefully adjusted on the composite DAPI images. For each marker, we measured at least two variables: the intensity of the signal (integrated absorbance) and the percentage of positive stained area, based on the binary images.

To determine activated ERK, we used both phosphorylated ERK and DAPI (binarized) images. By overlaying these, we were able to identify and count phosphorylated ERK-positive nuclei (a value that was normalized to the total number of nuclei in the area given by DAPI), whereas cytoplasmic phosphorylated ERK was obtained by subtracting nuclear phosphorylated ERK area from the total area that stained positive for phosphorylated ERK (total phosphorylated ERK) and normalizing it to the total area of the map. On the phosphorylated S6 binarized images, a closing operation was done (dilation followed by erosion) to fill in the unstained nuclear area (S6 being a cytoplasmic marker), so an estimate of the area of the cells that stained positive for phosphorylated S6 was obtained and that was normalized to the tumoral map area.

The cleaved caspase-3 and Ki-67 images were also binarized. To count the number of positive objects for the cellular markers, we used size criteria to eliminate the background and a mean value of a tumoral cell/nucleus area to resolve the clusters. Microvascular density was measured using CD31 staining. On the binarized image, a closing operation was done to fill the vascular lumen. For microvessel density (MVD), we introduced additional size and shape criteria to obtain the number and size distribution of the vessels.

Statistical Analysis

The markers of interest were phosphorylated S6, phosphorylated ERK, cleaved caspase-3, Ki-67, and MVD. Phosphorylated S6 and phosphorylated ERK were evaluated using both integrated absorbance values and percentage of positive area. The other markers were expressed as percentage of positive area. Phosphorylated ERK was also evaluated in cytoplasm as well as in the nucleus.

Because for each marker there were several sections analyzed within each tumor, the comparison between the treatment arms was made using the random effects model (a simple ANOVA test assumes that the records are independent; therefore, it is not appropriate for this data set). For each marker, the normality assumption of the residuals was visually inspected. The percentages of positive area for phosphorylated S6 and phosphorylated ERK were log transformed to fulfill the normality assumption of the residuals. The mean value for each marker and for each treatment was expressed as the least square means calculated using the model. When the marker was log transformed (phosphorylated S6 and phosphorylated ERK percentage of positive area), the means obtained from the model were back transformed to reflect the usual scale.

The analysis of the tumor growth was done using mixed models, considering a spatial correlation between the measurements for the same mouse over time.

Results

Rapamycin and Erlotinib Interact to Decrease the Level of S6 Phosphorylation following Stimulation with EGF *In vitro*

Continuous exposure of SiHa cells for 48 hours resulted in nonsignificant growth inhibition using a range of rapamycin and erlotinib concentrations, whereas the combination produced statistically significant inhibition determined by MTS assay ($P = 0.01$; Fig. 2). This was associated with a decrease in the percentage of cells in S phase. There was no increase in apoptosis, determined by flow cytometric analysis of cleaved caspase-3, under any of the *in vitro* treatments tested (data not shown).

Whereas MAPK is responsible mainly for relieving an inhibitory conformation of p70S6K, PI3K/PKB/mTOR ensures its complete activation (22, 26). Furthermore, phosphorylation of S6 at Ser^{235}/Ser^{236} sites is also the result of combined mTOR and MAPK signaling (29). As shown in Fig. 2, phosphorylation of ERK, Akt, p70S6K, and S6 was detectable in all three cell lines when these were grown in the presence of 10% fetal bovine serum. As expected, S6 phosphorylation (Ser^{235}/Ser^{236}) was suppressed by rapamycin at all concentrations tested, whereas treatment with the MAPK/ERK kinase inhibitor U0126 resulted in decreased phosphorylated ERK (Fig. 2). Although erlotinib also decreased ERK activation in all three cell lines, the effect on phosphorylated S6 was much less. Following EGF stimulation, both rapamycin and erlotinib partially suppressed phosphorylated S6 (Ser^{235}/Ser^{236}), whereas the two drugs combined produced almost complete inhibition in all three cell lines. Similar results

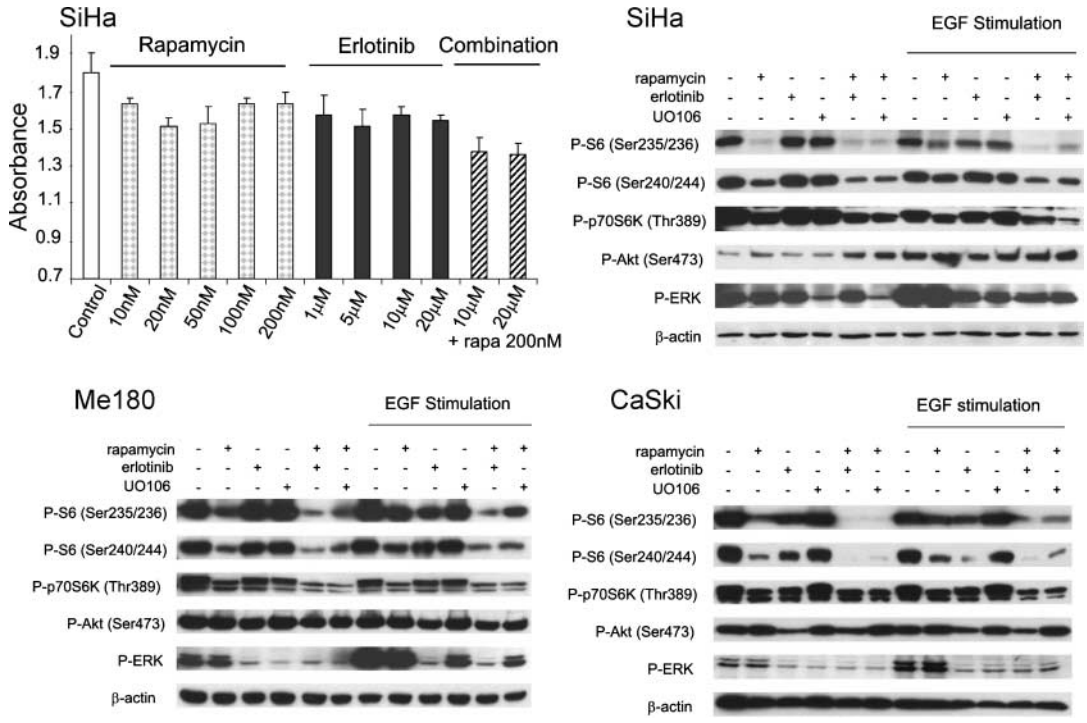

Figure 2. *Top left,* effects of 48 h of treatment with rapamycin or erlotinib at the indicated concentrations on the *in vitro* growth of SiHa cells. Rapamycin (200 nmol/L) was combined with erlotinib (10 or 20 mmol/L). *Columns,* mean of three separate experiments; *bars,* SE. Effects of inhibitors on downstream effectors of PI3K/PKB and MAPK signaling in SiHa, Me180, and CaSki cells *in vitro*. Cells were treated with rapamycin (50 nmol/L), erlotinib (20 μmol/L), or UO126 (10 μmol/L) as single agents or in combinations for 60 min and then activated with EGF (50 ng/mL) for 15 min where indicated. *P-S6,* phosphorylated S6; *P-p70S6K,* phosphorylated p70S6K; *P-Akt,* phosphorylated Akt; *P-ERK,* phosphorylated ERK.

were seen combining the MAPK/ERK kinase inhibitor UO126 with rapamycin. However, unlike erlotinib, UO126 alone did not significantly reduce phosphorylated S6 in EGF-stimulated cells nor had any effect on PKB/Akt phosphorylation. The activation of the other pair of serine sites on S6 (Ser^{240}/Ser^{244}) exhibited a pattern similar to Ser^{235}/Ser^{236} but showed greater sensitivity to rapamycin and erlotinib, consistent with these sites showing greater dependence on PI3K/PKB/mTOR relative to MAPK signaling (29).

In vivo Experiments

Effects of the Combined Therapy on Tumor Growth. As shown in Fig. 3, increased growth delay was seen in SiHa tumors treated with the combination of drugs when compared with either the control group ($P < 0.0001$) or single drug-treated animals ($P = 0.0002$ versus erlotinib; $P = 0.01$ versus rapamycin). Rapamycin alone had a statistically significant effect when compared with the controls ($P = 0.002$), whereas for erlotinib a trend was present ($P = 0.08$). There was no significant difference between rapamycin and erlotinib when considering the tumor progression. In terms of drug toxicity, although erlotinib-treated mice presented weight loss (between 7% and 13%), in the group that also received rapamycin the animals displayed an apparent overall healthier appearance.

In contrast to SiHa, treatment with erlotinib produced no significant effect on Me180 or CaSki tumor growth, but the combination of erlotinib plus rapamycin produced significantly greater growth delay in Me180 xenografts compared with rapamycin alone ($P = 0.02$). As shown in Fig. 3, CaSki tumors were highly responsive to rapamycin, and there was no additional benefit with the addition of erlotinib.

Effects of the Combined Therapy on S6 and ERK Activation *In vivo*

Western Blots. In preliminary experiments, the acute effects on signaling pathways were tested in SiHa xenografts by treating quadruplicate groups of animals with 2.5 mg/kg rapamycin, 10 mg/kg erlotinib, or the combination followed by sacrifice after 1 hour. Treatment with erlotinib resulted in a large decrease in phosphorylated ERK. Although there was a decrease in phosphorylated S6 following rapamycin, which was more pronounced with the combination, this effect was much

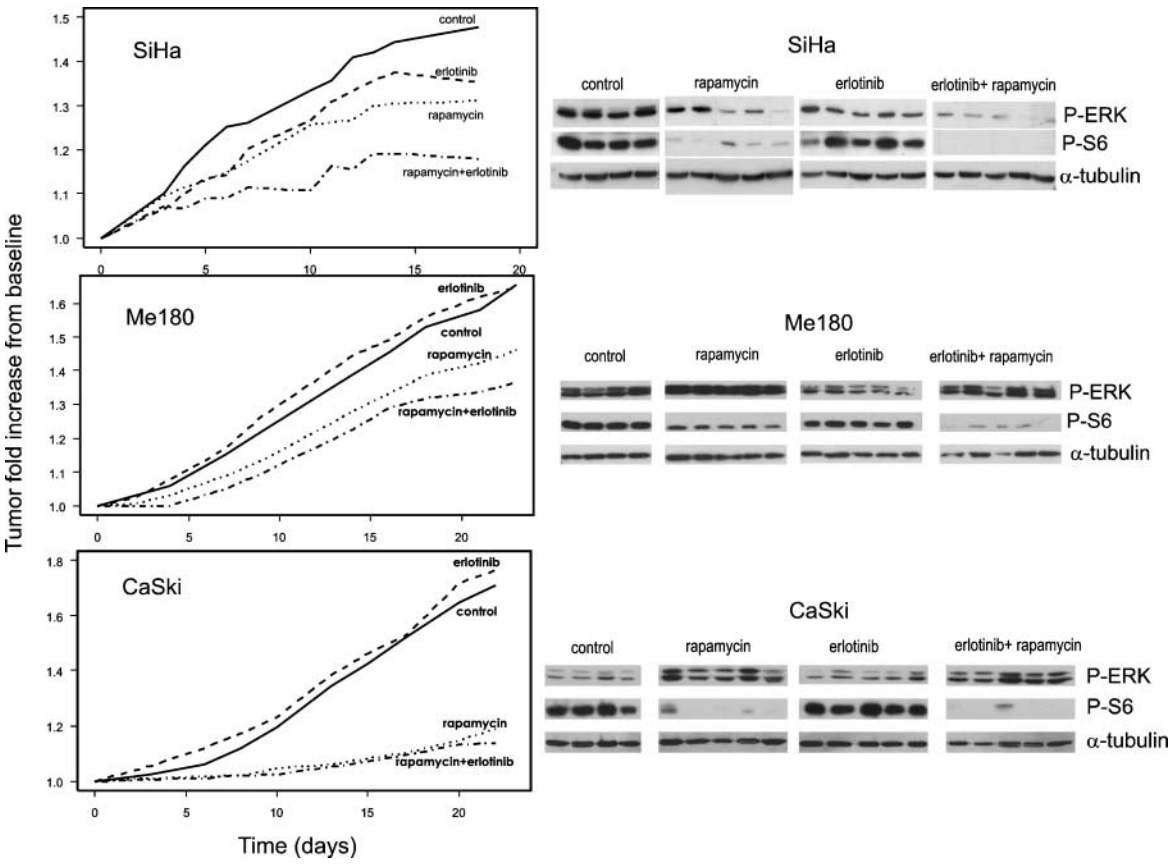

Figure 3. *Left,* tumor growth curves for SiHa (*top*), Me180 (*middle*), and CaSki (*bottom*) xenografts treated with rapamycin (2.5 mg/kg twice weekly), erlotinib (10 mg/kg daily), or the drug combination compared with drug vehicle control. The tumor plus leg diameter was measured periodically. *Lines,* defined by the average tumor increase measured at each time point. *Right,* corresponding Western blots obtained from the individual xenografts from each treatment group, probed for activated S6 and ERK.

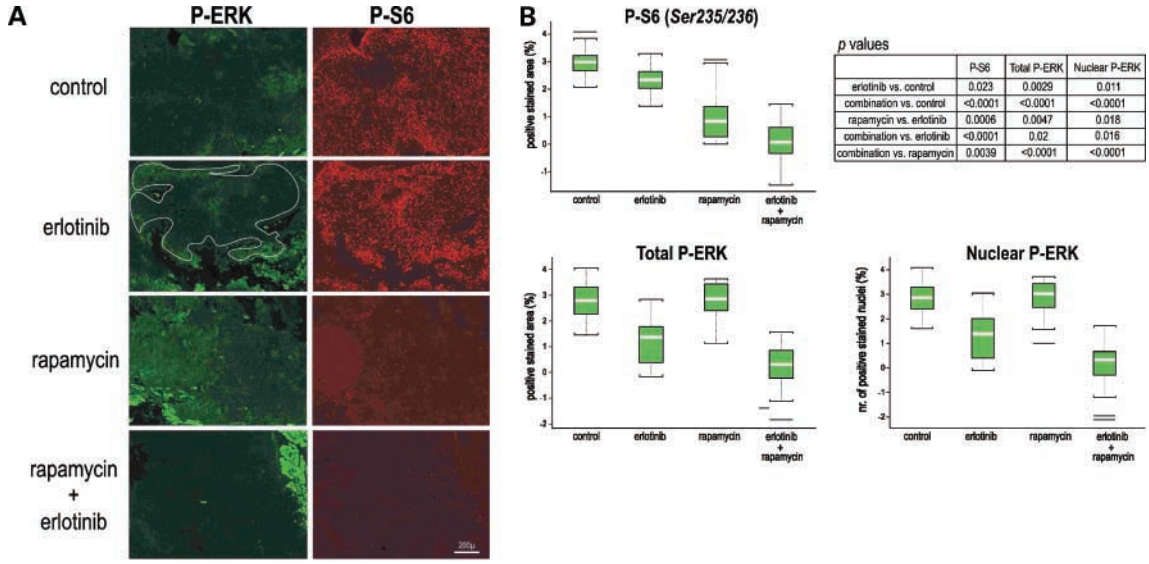

Figure 4. **A,** representative composite images (4 × 4 20× tiled fields) of tissue sections from SiHa xenografts, double stained for phosphorylated ERK (*green*) and phosphorylated S6 (*red*). Intratumoral heterogeneity is evident especially for phosphorylated ERK; the image from the erlotinib-treated animal displays the map of viable tumoral tissue in which the measurements were made. **B,** box and whiskers plots of phosphorylated S6 and phosphorylated ERK immunofluorescence staining analysis. Phosphorylated ERK was further subdivided into nuclear and cytoplasmic staining based on DAPI fluorescence.

less than that seen following 1 hour of drug exposure *in vitro* (data not shown). In contrast, in the 19-day continuous dosing experiments, phosphorylated S6 (Ser^{235}/Ser^{236}) was almost undetectable in the rapamycin-treated SiHa tumors, and any additional effect of erlotinib was not detectable by Western blot. Phosphorylated ERK suppression seemed similar in erlotinib alone treated mice and in the combined treatment group. Although ineffective in tumor growth delay, erlotinib produced decreased phosphorylated ERK in Me180 xenografts, associated with an enhanced effect of rapamycin on phosphorylated S6. Whereas CaSki cells grown in tissue culture showed decreased phosphorylated ERK following treatment with erlotinib (Fig. 2), this effect was not seen in the CaSki xenografts, and there was no enhancement of rapamycin on S6 phosphorylation (Fig. 3).

Immunofluorescence Staining. Tissue sections from the SiHa 19-day continuous treatment experiment were double immunostained for fluorescence image analysis of phosphorylated S6 (Ser^{235}/Ser^{236}) and phosphorylated ERK. Because these measurements were made only in the viable tumor areas, unlike the Western blot analyses, they exclude necrotic or nontumoral tissue. Decreased integrated absorbance values and positive pixel areas for phosphorylated S6 were found following treatment with either rapamycin or erlotinib, and this effect was greater with the combination of drugs (Fig. 4A). All of the differences were statistically significant (Fig. 4B). Total phosphorylated ERK, expressed as percentage of positive stained area, was less when tumors were treated with erlotinib compared with the controls and further decreased with the combination. By using a DAPI nuclear mask, we were also able to measure nuclear phosphorylated ERK and found that this followed the same distribution pattern as the total activated protein (Fig. 4B), whereas erlotinib treatment did not decrease cytoplasmic phosphorylated ERK (data not shown).

Drug Effects on Cellular Proliferation and Apoptosis

The Ki-67 labeling index obtained for the SiHa viable tumoral areas showed a significant decrease following rapamycin treatment ($P = 0.03$) but not with erlotinib ($P = 0.16$). No significant differences in cleaved caspase-3 staining in tumor tissue were seen between the groups (data not shown).

Drug Effects on MVD and VEGF Plasma Levels

The image analysis technique used to measure MVD is illustrated in Fig. 5A, and the results obtained from the SiHa continuous dosing experiment are shown in Fig. 5B. There was no significant effect using either of the single agents, but the combination of erlotinib and rapamycin resulted in a significant decrease in MVD ($P = 0.012$). To investigate the antiangiogenic effects of the drug combination further, we measured plasma VEGF levels following continuous dosing. As shown in Fig. 5C, there was a nonsignificant trend for lower VEGF in the erlotinib-treated group and a significant decrease in plasma VEGF following combined treatment ($P = 0.017$), consistent with the effects seen on MVD. We also tested plasma VEGF from the Me180 and CaSki groups of mice but found that this was not detectable above background.

Discussion

In recent years, EGFR inhibitors and rapamycin analogues have been extensively tested against human solid tumors. Each class of agent has been found to be well tolerated

and to produce clinical benefit in a wide range of tumor types. However, responses are typically seen only in a minority of patients and are often of short duration. Given the known interactions between signaling pathways downstream from EGFR and mTOR, we hypothesized that the combination of rapamycin plus erlotinib would show additive or synergistic effects *in vivo* and tested this in a series of human cervical squamous cell carcinoma cell lines. All three cell lines responded to rapamycin and erlotinib treatment *in vitro* with reduced phosphorylated S6 and phosphorylated ERK, respectively. SiHa and Me180 xenografts both showed enhanced tumor growth delay with the drug combination, associated with effects on signaling pathways that are consistent with our hypothesis.

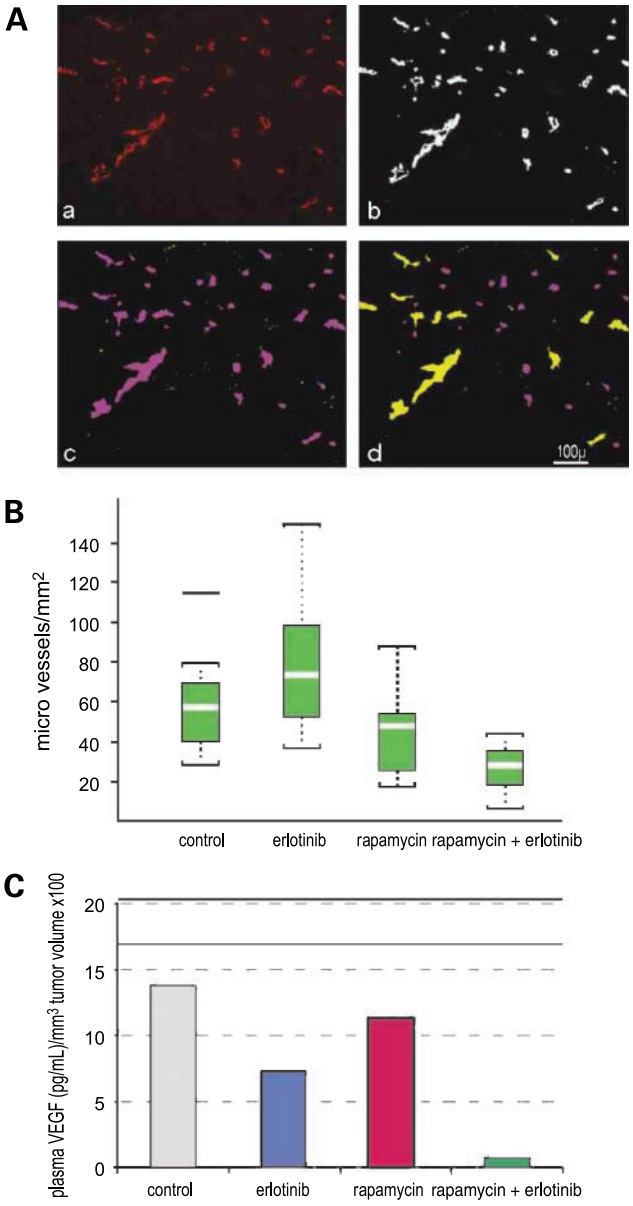

Figure 5. **A,** measuring MVD: composite images of CD31-stained tissue sections from the continuously treated animals (**a**) were further modified (**b** and **c**) to allow microvessel selection (**d**, *magenta objects*) based on size and shape criteria. **B,** box and whiskers plots showing *in vivo* effects of 19 d of drug treatment on microvascular density. **C,** effects of rapamycin and erlotinib on plasma VEGF concentrations in the same SiHa-bearing mice. Samples were obtained 1 hour after the last dose of drug, and VEGF concentration measured by ELISA was normalized to the tumor volume (width^2 × length / 2).

It is still unclear what dictates the response to EGFR inhibitors because the status of the receptor itself is not predictive (1, 2). On the other hand, rapamycin and analogues were repeatedly found to do better whenever PKB is constitutively activated (4, 8, 12–15, 36). The cervical carcinoma xenograft models were used because the tumors express EGFR and activated PKB. As well as Western blotting, wide-field multicolor fluorescence image analysis was used to study effects in SiHa xenografts because this has several advantages in studying biological processes at the tumor tissue level (37). Relative to immunohistochemistry, it is more quantitative, and it allows colocalization of multiple markers in the same tissue section. Moreover, in contrast to obtaining data from ''hotspots'' or randomly chosen fields, the use of composite, tiled field images allows the analysis of large tissue areas, which accounts for the heterogeneity of the tissue itself and of the markers of interest. In the present study, phosphorylated S6 (Ser^{235}/Ser^{236}) and phosphorylated ERK were chosen as the appropriate biomarkers to evaluate erlotinib and rapamycin effects on intracellular signaling. Although their levels correlated well in Western blots versus computerized image analysis, the latter measurements were evidently more accurate as they quantify activated proteins exclusively within the viable tumoral tissue.

In SiHa tumors, rapamycin given together with erlotinib had a significantly greater effect on tumor growth when compared with single drug alone, associated with enhanced suppression of phosphorylated S6, lower VEGF plasma levels, and decreased MVD, consistent with pathway interactions shown in Fig. 1. For some signaling inhibitors, it is difficult to discern *in vivo* between cytostatic/cytotoxic and antiangiogenic effects (14, 34). The mTOR and MAPK pathways regulate protein translation through the common targets p70/S6 ribosomal protein and 4E-BP/eIF-4E (5, 6, 24, 25). However, despite the significant decrease in phosphorylated S6, it is unlikely that the tumor growth delay can be explained entirely based on impaired translation. In the SiHa xenografts, there was a significant decrease in proliferation measured by Ki-67 labeling after rapamycin administration but not with erlotinib. We did not see major changes in apoptosis assessed by caspase-3 cleavage following 19 days of continuous dosing but cannot exclude the possibilities that the drug combination produces increased apoptosis at an earlier stage of treatment or induces a caspase-independent mode of tumor cell death (14, 34, 38).

In contrast to SiHa, erlotinib treatment did not produce significant tumor growth delay in Me180 xenografts despite a reduction in phosphorylated ERK. However, erlotinib enhanced the effects of rapamycin on tumor growth as well as on S6 phosphorylation. This finding supports the idea that the combination of rapamycin and an EGFR inhibitor might have clinical activity against cancers that are refractory to EGFR inhibitors. In contrast, CaSki cells, which were responsive to erlotinib *in vitro*, showed no effects on tumor growth or phosphorylated ERK when treated with this agent *in vivo*. These tumors were very responsive to rapamycin *in vivo*, but there was no additional effect when this was combined with erlotinib, consistent with its lack of effect on ERK and S6 phosphorylation *in vivo*. Although highlighting the complexity of combination treatment protocols that incorporate multiple signal transduction inhibitors, overall, the results reported here support the further clinical investigation of rapamycin and EGFR inhibitor combinations in the treatment of cancer patients.

Acknowledgments

We thank Melania Pintilie for the statistical analysis, Trudey Nicklee, May Cheung, Pinjiang Cao, and James Ho for excellent technical assistance, and Ken Iwata (OSI Pharmaceuticals) for his support and helpful comments.

References

1. Giaccone G. Epidermal growth factor receptor inhibitors in the treatment of non-small-cell lung cancer. J Clin Oncol 2005;23:3235 – 42.

2. Jimeno A, Hidalgo M. Blockade of epidermal growth factor receptor (EGFR) activity. Crit Rev Oncol Hematol 2005;53:179 – 92.

3. Albanell J, Codony-Servat J, Rojo F, et al. Activated extracellular signal-regulated kinases: association with epidermal growth factor receptor/transforming growth factor α expression in head and neck squamous carcinoma and inhibition by anti-epidermal growth factor receptor treatments. Cancer Res 2001;61:6500 – 10.

4. Bjornsti MA, Houghton PJ. The TOR pathway: a target for cancer therapy. Nat Rev Cancer 2004;4:335 – 48.

5. Hay N, Sonenberg N. Upstream and downstream of mTOR. Genes Dev 2004;18:1926 – 45.

6. Fingar DC, Richardson CJ, Tee AR, Cheatham L, Tsou C, Blenis J. mTOR controls cell cycle progression through its cell growth effectors S6K1 and 4E-BP1/eukaryotic translation initiation factor 4E. Mol Cell Biol 2004;24:200 – 16.

7. Arsham AM, Howell JJ, Simon MC. A novel hypoxia-inducible factor-independent hypoxic response regulating mammalian target of rapamycin and its targets. J Biol Chem 2003;278:29655 – 60.

8. Edinger AL, Linardic CM, Chiang GG, Thompson CB, Abraham RT. Differential effects of rapamycin on mammalian target of rapamycin signaling functions in mammalian cells. Cancer Res 2003;63: 8451 – 60.

9. Hudson CC, Liu M, Chiang GG, et al. Regulation of hypoxia-inducible factor 1α expression and function by the mammalian target of rapamycin. Mol Cell Biol 2002;22:7004 – 14.

10. Humar R, Kiefer FN, Berns H, Resink TJ, Battegay EJ. Hypoxia enhances vascular cell proliferation and angiogenesis *in vitro* via rapamycin (mTOR)-dependent signaling. FASEB J 2002;16:771 – 80.

11. Tee AR, Anjum R, Blenis J. Inactivation of the tuberous sclerosis complex-1 and -2 gene products occurs by phosphoinositide 3-kinase/Akt-dependent and -independent phosphorylation of tuberin. J Biol Chem 2003;278:37288 – 96.

12. Kenerson HL, Aicher LD, True LD, Yeung RS. Activated mammalian target of rapamycin pathway in the pathogenesis of tuberous sclerosis complex renal tumors. Cancer Res 2002;62:5645 – 50.

13. Zhong H, Chiles K, Feldser D, et al. Modulation of hypoxia-inducible factor 1α expression by the epidermal growth factor/phosphatidylinositol 3-kinase/PTEN/AKT/FRAP pathway in human prostate cancer cells: implications for tumor angiogenesis and therapeutics. Cancer Res 2000; 60:1541 – 5.

14. Guba M, von Breitenbuch P, Steinbauer M, et al. Rapamycin inhibits primary and metastatic tumor growth by antiangiogenesis: involvement of vascular endothelial growth factor. Nat Med 2002;8:128 – 35.

15. Neshat MS, Mellinghoff IK, Tran C, et al. Enhanced sensitivity of PTEN-deficient tumors to inhibition of FRAP/mTOR. Proc Natl Acad Sci U S A 2001;98:10314 – 9.

16. Mills GB, Lu Y, Kohn EC. Linking molecular therapeutics to molecular diagnostics: inhibition of the FRAP/RAFT/TOR component of the PI3K pathway preferentially blocks PTEN mutant cells *in vitro* and *in vivo*. Proc Natl Acad Sci U S A 2001;98:10031 – 3.

17. Vivanco I, Sawyers CL. The phosphatidylinositol 3-kinase AKT pathway in human cancer. Nat Rev Cancer 2002;2:489 – 501.

18. Blalock WL, Navolanic PM, Steelman LS, et al. Requirement for the PI3K/Akt pathway in MEK1-mediated growth and prevention of apoptosis: identification of an Achilles heel in leukemia. Leukemia 2003;17: 1058 – 67.

19. Davies CC, Mason J, Wakelam MJ, Young LS, Eliopoulos AG. Inhibition of PI3K and ERK MAPK-regulated protein synthesis reveals the pro-apoptotic properties of CD40 ligation in carcinoma cells. J Biol Chem 2004;279:1010 – 9.

20. Eisenmann KM, VanBrocklin MW, Staffend NA, Kitchen SM, Koo HM. Mitogen-activated protein kinase pathway-dependent tumor-specific survival signaling in melanoma cells through inactivation of the proapoptotic protein bad. Cancer Res 2003;63:8330 – 7.

21. Harada H, Andersen JS, Mann M, Terada N, Korsmeyer SJ. p70S6 kinase signals cell survival as well as growth, inactivating the pro-apoptotic molecule BAD. Proc Natl Acad Sci U S A 2001;98: 9666 – 70.

22. Krasilnikov M, Ivanov VN, Dong J, Ronai Z. ERK and PI3K negatively regulate STAT-transcriptional activities in human melanoma cells: implications towards sensitization to apoptosis. Oncogene 2003;22: 4092 – 101.

23. Lehman JA, Calvo V, Gomez-Cambronero J. Mechanism of ribosomal p70S6 kinase activation by granulocyte macrophage colony-stimulating factor in neutrophils: cooperation of a MEK-related, THR^{421}/SER^{424} kinase and a rapamycin-sensitive, m-TOR-related THR^{389} kinase. J Biol Chem 2003;278:28130 – 8.

24. Lehman JA, Gomez-Cambronero J. Molecular crosstalk between p70S6k and MAPK cell signaling pathways. Biochem Biophys Res Commun 2002;293:463 – 9.

25. Pende M, Um SH, Mieulet V, et al. S6K1(−/−)/S6K2(−/−) mice exhibit perinatal lethality and rapamycin-sensitive 5′-terminal oligopyrimidine mRNA translation and reveal a mitogen-activated protein kinase-dependent S6 kinase pathway. Mol Cell Biol 2004; 24:3112 – 24.

26. Nomura M, He Z, Koyama I, Ma WY, Miyamoto K, Dong Z. Involvement of the Akt/mTOR pathway on EGF-induced cell transformation. Mol Carcinog 2003;38:25 – 32.

27. Yu Y, Sato JD. MAP kinases, phosphatidylinositol 3-kinase, and p70 S6 kinase mediate the mitogenic response of human endothelial cells to vascular endothelial growth factor. J Cell Physiol 1999;178:235 – 46.

28. Semenza G. Signal transduction to hypoxia-inducible factor 1. Biochem Pharmacol 2002;64:993 – 8.

29. Sang N, Stiehl DP, Bohensky J, Leshchinsky I, Srinivas V, Caro J. MAPK signaling up-regulates the activity of hypoxia-inducible factors by its effects on p300. J Biol Chem 2003;278:14013 – 9.

30. Choe G, Horvath S, Cloughesy TF, et al. Analysis of the phosphatidylinositol 3′-kinase signaling pathway in glioblastoma patients *in vivo*. Cancer Res 2003;63:2742 – 6.

31. Romanelli A, Dreisbach VC, Blenis J. Characterization of phosphatidylinositol 3-kinase-dependent phosphorylation of the hydrophobic motif site Thr(389) in p70 S6 kinase 1. J Biol Chem 2002;277: 40281 – 9.

32. Vinals F, Chambard JC, Pouyssegur J. p70 S6 kinase-mediated protein synthesis is a critical step for vascular endothelial cell proliferation. J Biol Chem 1999;274:26776 – 82.

33. Sini P, Wyder L, Schnell C, et al. The antitumor and antiangiogenic

activity of vascular endothelial growth factor receptor inhibition is potentiated by ErbB1 blockade. Clin Cancer Res 2005;11:4521 – 32.

34. Liu M, Howes A, Lesperance J, et al. Antitumor activity of rapamycin in a transgenic mouse model of ErbB2-dependent human breast cancer. Cancer Res 2005;65:5325 – 36.

35. Pore N, Liu S, Haas-Kogan DA, O'Rourke DM, Maity A. PTEN mutation and epidermal growth factor receptor activation regulate vascular endothelial growth factor (VEGF) mRNA expression in human glioblastoma cells by transactivating the proximal VEGF promoter. Cancer Res 2003;63:236 – 41.

36. Gera JF, Mellinghoff IK, Shi Y, et al. AKT activity determines sensitivity to mTOR inhibitors by regulating cyclin D1 and c-*myc* expression. J Biol Chem 2004;279:2737 – 46.

37. Hedley D, Pintilie M, Woo J, et al. Up-regulation of the redox mediators thioredoxin and apurinic/apyrimidinic excision (APE)/Ref-1 in hypoxic microregions of invasive cervical carcinomas, mapped using multispectral, wide-field fluorescence image analysis. Am J Pathol 2004; 164:557 – 65.

38. Castedo M, Ferri KF, Kroemer G. Mammalian target of rapamycin (mTOR): pro- and anti-apoptotic. Cell Death Differ 2002;9:99 – 100.